Electronic Supplementary Information

Green synthesis of carbon dots using expired agar for a label-free fluorescence signal-amplified detection of ferric ion utilizing oxalate functionalization

O. J. Achadu[a,b*], G. Elizur[c], B. E. ThankGod[d], E. Y. Park,[e,f]

a. Department of Chemistry, University of Warwick, CV4 7AL, United Kingdom.
b. Institute of Advanced Study, University of Warwick, CV4 7AL, United Kingdom.
c. International Study Centre, University of Strathclyde, Glasgow, United Kingdom.
d. Engineering and Physical Sciences, University of Southampton, United Kingdom.
e. Research Institute of Green Science and Technology, Shizuoka University, 836 Ohya, Suruga-ku, Shizuoka 422-8529, Japan.
f. Laboratory of Biotechnology, Department of Bioscience, Graduate School of Science and Technology, Shizuoka University, 836 Ohya Suruga-ku, Shizuoka 422-8529, Japan.

E-mail:
Ojodomo.Achadu@warwick.ac.uk (OJA)

Results and discussion cont'd

S1. ag-oxCDs synthesis optimization protocol

It is well known that carbonization process for CDs preparation is strongly influenced by temperature and that the experimental conditions of hydrothermal process are critical in terms of ensuing optical properties. Indeed, from our experimental optimizations, temperatures of 160 °C and above were those that could form smaller nanoparticles (<10 nm) containing carbogenic and/or graphitic domains.

Conversely, lower temperatures (typically below 160 °C) resulted in weakly fluorescing nanoparticles which were not stable in aqueous medium. We think that this temperature resulted in the incomplete condensation and dehydration reactions and not properly forming carbogenic fluorescent sites or domains. Following this, we decided to stick to the optimized hydrothermal conditions, heating temperature and time of 160 °C and 6 h to avoid under or over carbonization process, as the case may be. Details of different temperatures (typically above 160 °C) on the formation of the ag-oxCDs as investigated are shown in Fig. S1 presenting the TEM images of the hydrothermal treatments of PDA at 180 °C and 200 °C, respectively. The respective particle size distribution histograms shown in the insets (Fig. S1), indicate that there are different kinds of nanoparticles with some having very large diameters ranging from >10 - 30 nm, respectively. Meanwhile, the ag-oxCDs obtained at a lower temperature (optimized 160 °C) have a more uniform morphology and smaller particle size (shown in Fig. 1d in the main text), which shows the suitability of this hydrothermal heating temperature/time on the formation of the ag-oxCDs.

To further ascertain the difference in the quality of the CDs produced at the different hydrothermal conditions, the fluorescence quantum yields (QYs) were respectively evaluated for ag-oxCDs synthesized at 160 °C, 180 °C, 200 °C and for pristine ag-CDs (without oxalate moieties,

@160 ^{0}C). As shown in Table S1, the optimum QY was ascertained for ag-oxCDs @160 ^{0}C which informed our adoption of the ag-oxCDs (@160 ^{0}C) for further use in the Fe(III) detection.

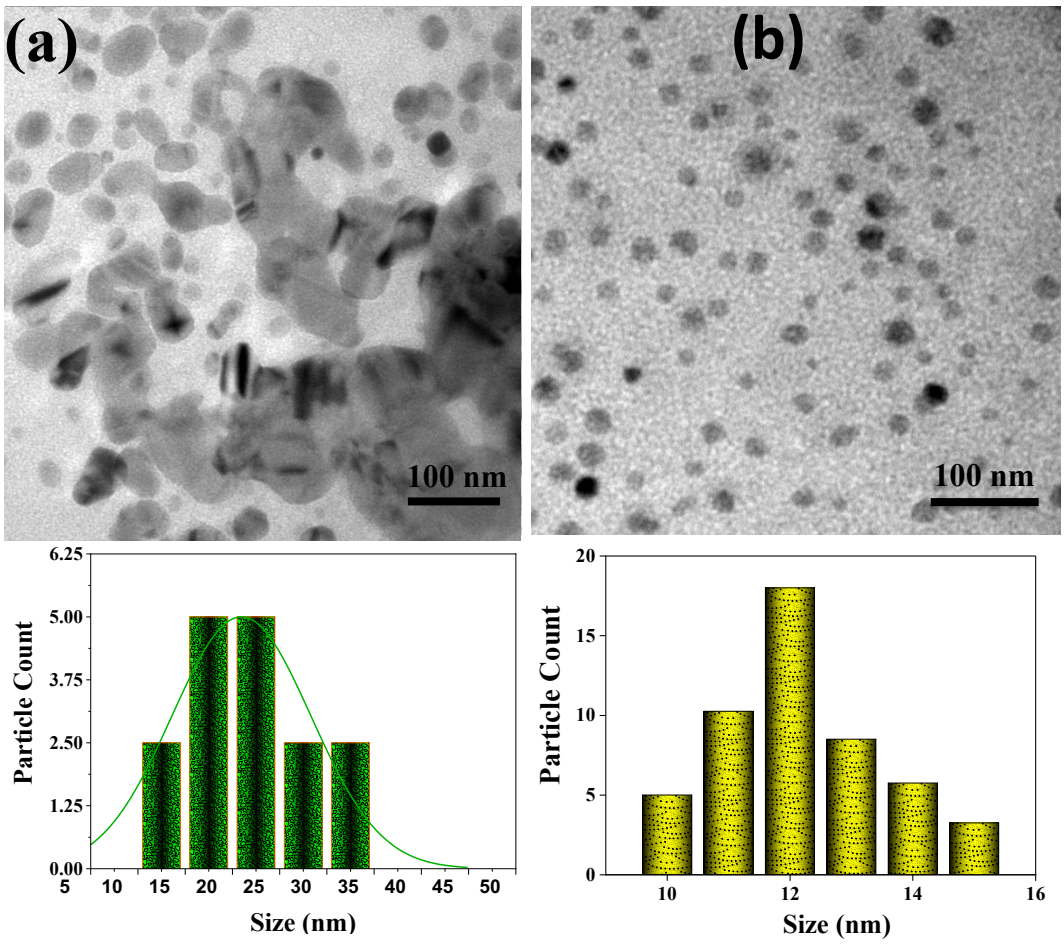

Fig. S1. TEM images of the hydrothermal treatment of the precursor PDA at (a) 180 ^{0}C and (b) 200 ^{0}C showing larger particles sizes. The corresponding histograms of the TEM images are shown.

Table S1. The fluorescence quantum yields calculated for the various agar-derived oxalate-CDs (pristine CDs) at different hydrothermal temperature.

Temperature	Quantum yield (%)
160 ^{0}C	32
180 ^{0}C	27
200 ^{0}C	25
AgCDs (no oxalate)	14

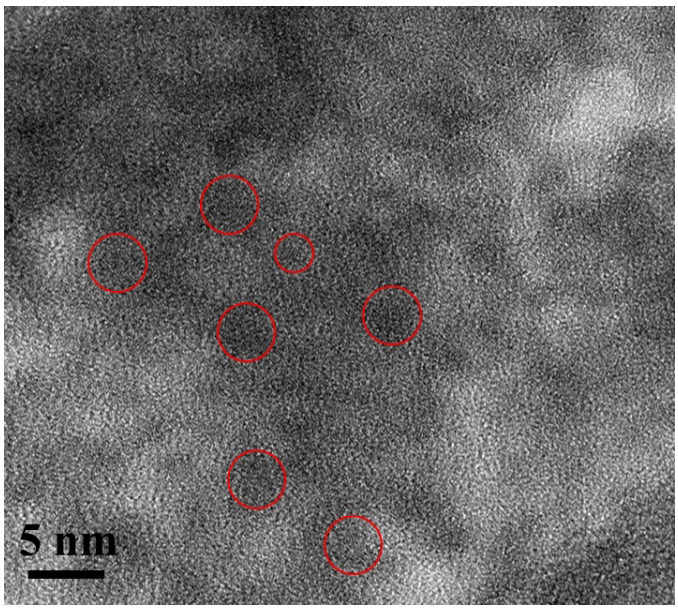

Fig. S2. HRTEM micrograph of ag-oxCDs with no clearly discernible lattice fringes which indicates a poor crystalline/graphitic feature of the CDs. Poorly crystalline and non-graphitic CDs have been reported previously[1,2].

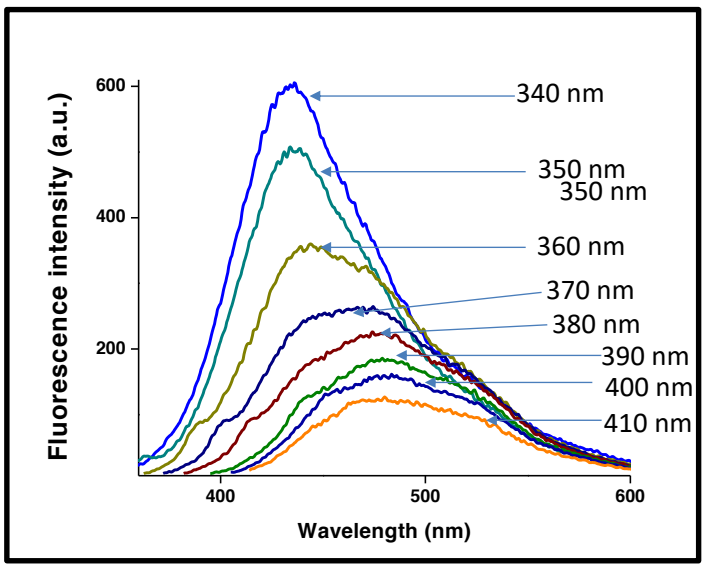

Fig. S3. Emission spectra of ag-oxCDs recorded at different excitation-wavelengths (340-410 nm) showing the excitation wavelength-dependent emission behaviour of ag-oxCDs.

Table S2. The LODs for Fe(III) detection based on CDs synthesized from other natural source precursors compared with agar-derived oxalate-CDs.

Carbon dots (QY,%)	Precursor	LOD (μM)	Reference
GSH-CDs (4 %)	Citric acid/Urea	0.1	[3]
N-CDs (14 %)	*Phyllanthus acidus*	0.9	[4]
N-CDs (9 %)	*Chionanthus refusus*	70	[5]
HN-CDs (23 %)	Dwarf Banana peel	0.66	[6]
CB-CDs (10.85 %)	Cranberry beans	9.55	[7]
W/E-CDs (~18 %)	Papaya	0.29/0.4	[8]
N-CDs (23.4 %)	Rice residue	0.7462	[9]
FW-CDs (22 %)	Food waste	32	[10]
C-dots (-)	Blueberries	9.97	[11]
CDs (-)	Cherry Plum	5	[12]
Ag-oxCDs (32 %)	Expired Agar	0.075	This work

99 **Table S3.** Practical detection of Fe(III) in spiked human serum and water samples using ICP-OES as
100 a reference technique. The quantified Fe (III) is shown with the recoveries and relative standard
101 deviations (RSDs)

Sample	Added Fe^{3+}, μM*	Detected Fe^{3+}, μM	Recovery % (n = 3)	RSD (%)
Spiked water	1.0 (1.15)	1.04	104±1.5	3.50
	10 (9.8)	10.1	101±1.8	1.25
	20 (20.5)	19.8	99±1.5	0.50
	50 (50.3)	50.05	100.1±0.52	1.43
	100 (100.5)	98.50	98.5±1.88	3.01
Human serum	1.00 (1.2)	1.02	102±1.6	2.45
	10 (10.3)	9.9	99±0.96	0.75
	20 (20.2)	19.72	98.6±0.38	2.34
	50 (49.6)	50.1	100.2±0.7	1.20
	100 (99.36)	99.80	99.8±1.3	0.98

102 * Obtained results from elemental analyses using ICP-OES

103

Reference:

1. J. Hou, J. Dong, H. Zhu, X. Teng, S. Ai and M. Mang, *Biosens. Bioelectron.*m 2015, 68, 20-26.
2. J. Wei, X. Zhang, Y. Sheng, J. Shen, P. Huang, S. Guo, J. Pan, B. Liu and B. Feng, *New J. Chem.*, 2014, 38, 906-909.
3. C. Wang, K. Jiang, Z. Xu, H. Lin and C. Zhang, *Inorg. Chem. Front*., 2016, 3, 514-522.
4. R. Atchudan, T.N.J.I. Edison, K. R. Aseer, S. Perumal, N. Karthik, and Y. R. Lee, *Biosens Bioelect*, 2018, 99, 303-311.
5. R. Atchudan, T.N.J.I. Edison, D. Chakradhar, S. Perumal, J.J. Shim and Y. R. Lee, *Sensors and Actuators B: Chemical*, 2017, 246, 497-509.
6. R. Atchudan, T.N.J.I. Edison, S. Perumal, N. Muthuchamy, and Y. R. Lee, *Fuel*, 2020, 275, 117821.
7. M. Zulfajri, G. Gedda, C.J. Chang, Y. P. Chang and G. G. Huang, *ACS Omega*, 2019, 4, 15382-15392.
8. N. Wang, Y. Wang, T. Guo, T. Yang, m. Chen, J. Wang. *Biosens Bioelect*, 2016, 85, 68-75.
9. H. Qi et al., J. Colloid & Interf. Sci., 2019, 539, 332-341.
10. J. Ahn et al., Mater. Sci. & Eng. C, 2019, C102, 106-112.
11. A. M. Aslandas, N. Balci, M. Arik, H. Sakiroglu, Y. Onganer, K. Meral, Appl. Surf. Sci., 2015, 356, 747-752.
12. H. Ma et al., Spectrochim. Acta Part A: Mol. and Biomol. Spect., 2019, 213, 281-287.